Coulomb localization in orbital degenerate, doped Mott insulators

Adolfo Avella,[1,2,3,a] Andrzej M. Oleś,[4,5] and Peter Horsch[5]
[1]*Dip. di Fisica "E.R. Caianiello", Università di Salerno, I-84084 Fisciano (SA), Italy*
[2]*CNR-SPIN, UOS Salerno, I-84084 Fisciano (SA), Italy*
[3]*Unità CNISM di Salerno, Università di Salerno, I-84084 Fisciano (SA), Italy*
[4]*M. Smoluchowski Institute of Physics, Jagiellonian University, PL-30348 Kraków, Poland*
[5]*Max-Planck-Institut für Festkörperforschung, Heisenbergstr. 1, D-70569 Stuttgart, Germany*

(Received 5 June 2018; accepted 21 August 2018; published online 6 September 2018)

We study electron localization in a three-band extended Hubbard model describing the t_{2g} electrons of doped vanadium perovskites such as $La_{1-x}Ca_xVO_3$, where Ca defects are represented by Coulomb potentials. The main goal of this paper is to explore what happens when long-range electron-electron (*e-e*) interactions are switched on. The electronic structure of these doped Mott-Hubbard insulators is calculated using the unrestricted Hartree-Fock approximation that allows to perform the required statistical averages over many distinct defect realizations. The Mott gap is found to persist up to large doping and the defect states, appearing inside of it, are seen to develop a defect states gap centered at the Fermi energy. The *internal* kinetic energy of the doped holes, forming spin-orbital polarons bound to the defects, induces the defect states gap even in the absence of *e-e* interactions. Such kinetic gap survives disorder fluctuations and is amplified by long-range *e-e* interactions. A study of the inverse participation ratio reveals the small size of such spin-orbital polarons and provides an explanation for the persistence of spin and orbital order up to high doping. https://doi.org/10.1063/1.5042829

I. INTRODUCTION

Doping Mott insulators has become a central topic of condensed matter physics with the discovery of high-T_c superconductivity.[1] We explore the effect of disorder of charged defects on the electronic excitations observed in the photoemission spectra of doped vanadium perovskites such as $La_{1-x}Ca_xVO_3$. Characteristic for the vanadium d^2 perovskites with partly filled t_{2g} valence orbitals is the persistence of the Mott insulating state and of spin and orbital order up to high concentrations x of Ca ions and doped holes[2–4] in striking contrast to cuprate superconductors. In these latter, e_g orbitals are largely split, and the doped holes, already at quite low concentrations, destroy the antiferromagnetic (AF) order and let the system metallize.[1]

The cubic vanadates are fascinating for several reasons, already the undoped compounds reveal a rich phase diagram with several spin- and orbitally- ordered phases, a pure orbitally-ordered phase and an orbitally-disordered high-temperature phase.[2,5] Interestingly, these almost perfect cubic systems show quasi-one-dimensional magnetic properties, as a result of strong orbital quantum fluctuations (OQF)[6] triggered by a weakly broken cubic symmetry, which is manifest in a preferred occupation of *xy* orbitals.[7] Strong OQF are a characteristic of the *C*-type AF (*C*-AF) spin and *G*-type alternating orbital (*G*-AO) ordered phase,[6] i.e., leading to a strong ferromagnetic (FM) exchange interaction along the *c*-axis. It was found for several compounds that the *C*-AF spin and *G*-AO phase is stable up to high doping,[2–4] for instance, up to $x \approx 0.2$ in $La_{1-x}Ca_xVO_3$ and $x \approx 0.5$ in $Y_{1-x}Ca_xVO_3$. Strong OQF

[a]Corresponding author: Adolfo Avella (avella@sa.infn.it)

and the robustness of G-AO correlations in the presence of defects appears unexpected at first glance. One explanation proposes that charged Ca defects support orbital singlet dimers in combination with the FM correlations along c and thereby they stabilize C-AF spin and G-AO correlations over the complementary G-AF spin and C-AO phase.[8]

In a recent study of the doped Mott insulating state of cubic vanadates based on a three-band Hubbard model,[9,10] it was shown that the Hubbard gap as well as the spin-orbital order are robust for moderate to high doping concentrations.[10,11] Moreover, the investigated model includes the Coulomb potentials of Ca defects as well as the long-range e-e interactions. It was further shown that the defect states, which are expected to appear in the Mott-Hubbard gap, form a soft defect states gap in the vicinity of the chemical potential.

In this article, we explore the evolution of the density of states (DOS) and of the emerging defect states, and, in particular, the variation of the defect states gap as functions of the strength of e-e interactions. Moreover, we shall contrast the Coulomb gap[12] obtained for the one-band Coulomb glass (CG) model to the multi-band physics in vanadates where both kinetic energy and e-e interactions determine the defect states gap. It is this latter feature that results in non-universal exponents that characterize the defect states gap in the multi-band system. Finally, we explore the degree of localization for all unrestricted Hartree-Fock (uHF) single particle states. This is achieved by an investigation of the spectral function representing the inverse participation number (IPN). The IPN reveals, in particular, a discontinuity of the localization of defect states at the chemical potential.

II. MODEL

The three-band model describing the t_{2g} electrons in doped vanadium $(La,Y)_{1-x}Ca_xVO_3$ perovskites,

$$\mathcal{H}_{t2g} = \mathcal{H}_{\rm Hub} + \eta \sum_{i\neq j} v(r_{ij}) n_i n_j + \sum_{m,i} v(r_{mi}) n_i, \tag{1}$$

includes the extended degenerate Hubbard model $\mathcal{H}_{\rm Hub}$, which involves the kinetic energy of t_{2g} electrons $\propto t$ and the intra-atomic Coulomb (Hubbard-Hund) interactions, i.e., those responsible for the multiplet splitting of V ions.[9] This model includes also the crystal field splitting and Jahn-Teller terms,[8] which we do not discuss here, see Refs. 8, 10, and 11.

Central for the physics of the doped system is the long-range Coulomb interaction

$$v(r) = \frac{e^2}{\varepsilon_c r}, \tag{2}$$

which determines e-e interactions that are defined in Eq. (1) as $\eta v(r_{ij})$, where r_{ij} is the distance between electrons at vanadium ions at sites i and j, respectively. The prefactor η can be tuned between 0 and 1 to analyze the relevance and the overall effects of these interactions. The operator n_i represents the total electron density at the V ion at site i. The third term in Eq. (1) represents the defect potentials $v(r_{mi})$, where $r_{mi} = |\mathbf{r}_m - \mathbf{r}_i|$ is the distance between a Ca defect at site m and the electrons at a V ion at site i; the closest distance is d. This interaction is repulsive (for electrons) as a Ca^{2+} ion has effectively a *negative* charge relatively to the La^{3+} or Y^{3+} ion that it substitutes. As a consequence, all electron states of V ions close to a defect, i.e., on a *defect cube*, are moved to higher energies, and doped holes are attracted by the Ca defects. The interaction $v(r)$ is screened by the dielectric constant of core electrons ε_c, which, for the vanadium perovskites, assumes a typical value[8] $\varepsilon_c \simeq 5$. Here, we shall introduce as parameter for the potential strength, instead of ε_c, the potential energy $V_D = v(d)$ of an electron at a V ion belonging to a defect cube. This parameter has been chosen equal to $V_D = 1.0$ eV.[11]

Next, we characterize the terms that contribute to the extended Hubbard model $\mathcal{H}_{\rm Hub}$. The kinetic energy of t_{2g} electrons between V ions results from a two-step process via intermediate oxygen $2p_\pi$ orbitals due to finite $d-p$ hybridization. The effective $d-d$ hopping is thus diagonal in the orbital flavor and vanishes in one of the three cubic directions that gives interesting consequences for the behavior of t_{2g} orbital polarons.[13] Accordingly, it is convenient to introduce the following short-hand notation for t_{2g} orbitals:[6] $|a\rangle \equiv |yz\rangle$, $|b\rangle \equiv |zx\rangle$, $|c\rangle \equiv |xy\rangle$. Here the label $\gamma = a, b, c$ refers to the

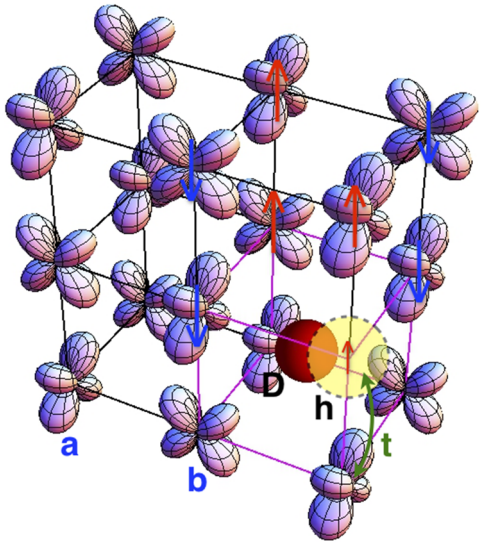

FIG. 1. Schematic picture of a *defect cube* (magenta) of V ions within C-AF spin (shown on a representative cube above the defect cube) and G-AO order of $\{a, b\}$ orbitals, called also CG order. A defect cube has a Ca ion with a (negative) effective charge in the center (D) and a doped hole (h), represented by a transparent yellow circle and by the (reduced) spin of the c orbital (not shown). The hole moves by hopping t along the FM vertical bond (green arrow).

cubic axis excluded from the hopping for the flavor γ; for the other two flavors the hopping along the nearest-neighbor bond $\langle ij\rangle \parallel \gamma$ is t, i.e.,

$$H_{\rm kin} = -t \sum_{\substack{\langle ij\rangle \parallel \gamma \\ \alpha\neq\gamma,\sigma}} \left(d^{\dagger}_{i\alpha\sigma} d_{j\alpha\sigma} + d^{\dagger}_{j\alpha\sigma} d_{i\alpha\sigma} \right). \tag{3}$$

Both $\{a, b\}$ orbitals are active along the c axis and this hopping is triggered when a Ca^{2+} defect injects a hole in the defect cube. Figure 1 shows a typical spin-orbital configuration in the host and around a Ca defect. The hole is confined to the defect cube by the potential $\propto V_D$ and prefers to hop along the vertical FM bond in agreement with double exchange.[10]

Strong correlations are the effect of the on-site Coulomb interactions between the electrons in t_{2g} orbitals,

$$\begin{aligned} \mathcal{H}_{\rm Hub} = H_{\rm kin} &+ \sum_{i,\mu<\nu} \left(U - \frac{5}{2} J_H \right) n_{i\mu} n_{i\nu} \\ &+ U \sum_{i\mu} n_{i\mu\uparrow} n_{i\mu\downarrow} - 2J_H \sum_{i,\mu<\nu} \vec{S}_{i\mu} \cdot \vec{S}_{i\nu} \\ &+ J_H \sum_{i,\mu\neq\nu} d^{\dagger}_{i\mu\uparrow} d^{\dagger}_{i\mu\downarrow} d_{i\nu\downarrow} d_{i\nu\uparrow}. \end{aligned} \tag{4}$$

Here we use the rotational invariant form of the Hubbard-Hund interaction,[9,10] where $n_{i\mu} = \sum_{\sigma} n_{i\mu\sigma}$ is the electron density operator in orbital $\mu = a, b, c$, U is intraorbital Coulomb repulsion, and J_H is the interorbital (Hund's) exchange elements for t_{2g} orbitals. Below we adopt $U = 4$ and $J_H = 0.6$, both in eV.[11] All other parameters are chosen as well as in set B of Ref. 11.

III. RESULTS

The system with charged defects is investigated using the uHF approximation for all interactions. Given the HF factorization, the electronic structure of the disordered system is calculated exactly. An important feature of the uHF method is that it yields two classes of states, namely the electron removal states, i.e., corresponding to the occupied single particle states, and the electron addition states. Therefore, one can directly identify the occupied states with the PhotoEmission States (PES)

and the unoccupied states with the Inverse PhotoEmission States (IPES). In presence of disorder, the density of states $N(\omega)$ is determined as statistical average over M distinct defect realizations with fixed concentration x:

$$N(\omega) \equiv \frac{1}{M}\sum_{s=1}^{M} N_s(\omega), \qquad N_s(\omega) = \frac{1}{6N}\sum_{n=1}^{6N} \delta(\omega - \omega_{n,s}), \tag{5}$$

where $\omega_{n,s}$ is the energy of the eigenstate n in the defect realization s and N is the number of sites in the system. The prefactor 6 is due to the 3-fold orbital ($|xy\rangle$, $|xz\rangle$, $|yz\rangle$) and the 2-fold spin degeneracy, i.e., to the total number of available states per site. In Fig. 2, we display a zoom of $N(\omega)$ between the lower Hubbard band (LHB) and the lowest part of the upper Hubbard band (UHB) for different *e-e* interaction strengths $\eta \in [0, 1]$ at doping $x = 0.10$. $N(\omega)$ reveals the full multiplet structure typical for an isolated V ion in its d^2 configuration, that is, it reflects the ionic character of the strongly correlated state. As a result of the strong local interactions, the distance of the centers of LHB and high-spin (HS) band is $U - 3J_H$, i.e., the same value as for an isolated ion.

For a charge neutral system ($\eta = 1$), we see that the LHB and the lowest component of the UHB, the HS state, are relatively narrow, whereas in the absence of *e-e* interactions ($\eta = 0$) these states are strongly broadened. This is due to the fact that at $\eta = 1$ defects and holes act together as dipoles, which reduces the impact of the disorder. In absence of *e-e* interactions ($\eta = 0$), the uncompensated Coulomb fields of defects amplifies the effect of disorder. Yet in both cases we observe a clear depletion of states at the chemical potential μ at $\omega = 0$; i.e., for $\eta = 1$ a soft gap that changes into an approximately linear pseudo-gap at $\eta = 0$. We note that in the latter case the gap is exclusively due to the kinetic energy.[11] We shall explore the precise character and variation of the defect states gap by a statistical analysis in the following.

We follow here Ref. 11 where it has been shown that the exponent ν characterizing the DOS $N(\omega) \propto \omega^{\nu}$ at the chemical potential can be determined from the statistical distribution of the gaps Δ_s corresponding to the distance between the lowest electron addition and the smallest electron removal energies for the defect realization s. The distribution of gaps Δ_s is described by a Weibull function, $f_{\rm W}(\omega; k, \lambda) = k/\lambda(\omega/\lambda)^{k-1} e^{-(\omega/\lambda)^k}$ for $\omega \geq 0$ and $f_{\rm W}(\omega; k, \lambda) = 0$ for $\omega < 0$, with parameters k and λ, where $\nu = k - 1$ determines the exponent of the defect states gap.

Figure 3 shows the behavior of parameters k and λ as functions of η. For $\eta = 0$, we find $\nu \simeq 1.0$, consistent with the linearity seen for $N(\omega)$ in Fig. 2. The statistical analysis tells us more, namely that in fact $N(0) = 0$. With increasing *e-e* interactions the linear defect states gap at $\eta = 0$ changes

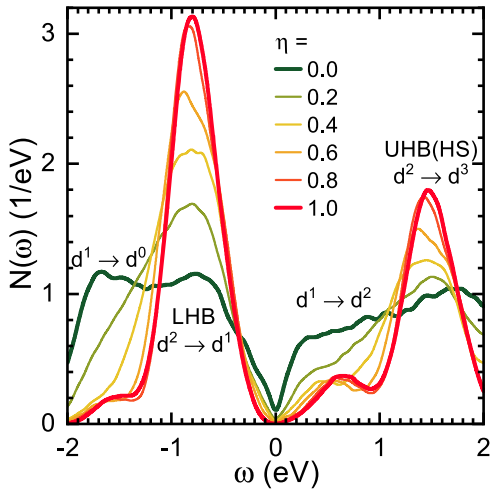

FIG. 2. Zoom of $N(\omega)$ (5) displaying the variation of the LHB ($d^2 \rightarrow d^1$) and of the lowest state of the UHB multiplet ($d^2 \rightarrow d^3$), the high-spin (HS) state, as function of the strength of *e-e* interactions η. Defect states in PES and IPES related to doped holes are marked as $d^1 \rightarrow d^0$ and $d^1 \rightarrow d^2$ transitions. The chemical potential μ is at $\omega = 0$. Results obtained by uHF for $8 \times 8 \times 8$ clusters, doping $x = 0.10$ averaging over 100 random defect realizations.

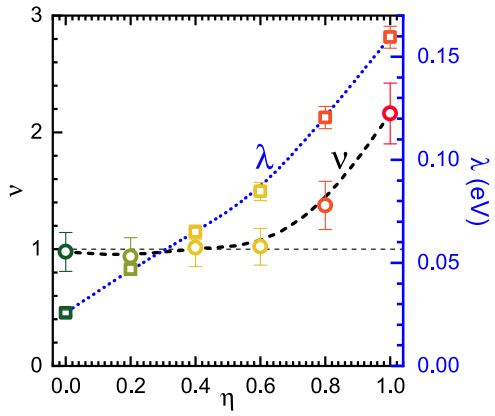

FIG. 3. Exponent ν (black, left) and scale parameter λ (blue, right) determined from a Weibull function that describes the distribution of smallest energy gaps Δ_s across the chemical potential. The η scale modulates the strength of *e-e* interactions, see Eq. (1).

gradually into a soft gap with $\nu \simeq 2$ at $\eta = 1$. One recognizes that the increasing size of the defect states gap is reflected by an increase of the scale parameter λ.

It is worth noting that the atomic limit ($t \to 0$) of (1) does not correspond exactly to the CG, at least not in the version of Efros and Shklovskii (ES),[12] not only because of the one-orbital to multi-orbital different characteristic of the model under analysis, but mainly because of the way disorder is implemented. In the CG model, disorder is represented by a random level distribution, whereas in the multi-band model used here (1), the random defect potentials, that lead to the random level distribution, appear explicitly. The most important consequence of this subtle difference is that the switching on of *e-e* interactions leads, for the charge neutral case $\eta = 1$, to overall dipolar interactions between the defect cube complex (defect + hole) and the electrons in the material, whereas in the CG model, the interactions are always monopolar. Moreover, the strong electronic correlations, leading to the doping of a Mott insulator and not of a simple metal, set the chemical potential in the upper tail of the LHB, where the density of states simply cannot be approximated by a constant as in the CG construction of ES. Altogether, these very facts lead to non-universal exponents $\nu = k - 1$ determined by the Weibull distribution function, instead of what happens to the CG exponent, as computed by ES, $\nu = d - 1$, which is determined uniquely by the spatial dimensionality d.

The defect states gap is a clear signature of localization. We shall determine the degree of localization of the uHF electronic wave functions $\psi_{n,s}$, related to the eigenstate n in the defect realization s. A useful measure is the IPN[14] that, for systems with spin and orbital degrees of freedom, reads as[11]

$$P_{n,s}^{-1} = \sum_i \left(\sum_{\alpha,\sigma} |\langle \psi_{n,s} | i, \alpha, \sigma \rangle|^2 \right)^2, \tag{6}$$

where the internal sums in α and σ are over local orbital and spin degrees of freedom, respectively, while the remaining sum in i is over N. $\psi_{n,s}$, is assumed to be normalized, i.e., $\sum_{i,\alpha,\sigma} |\langle \psi_{n,s} | i, \alpha, \sigma \rangle|^2 = 1$. This definition is such that the participation number $P_{n,s}$ (bound to be $P_{n,s} \geq 1$) is $P_{n,s} = 1$ only if the wave function is localized on a single site, while for a Bloch state returns $P_{n,s} = N$. More insight into the nature of the electronic states near and far from the Fermi energy (at μ_s for sample s and $\omega = 0$ for the average) may be gained by analyzing the evolution of the spectral function related to IPN[11] on increasing energy ω across the chemical potential,

$$P^{-1}(\omega) \equiv \frac{1}{M} \sum_{s=1}^{M} \left[\frac{1}{N_s(\omega)} \sum_{n=1}^{6N} P_{n,s}^{-1} \delta(\omega - \omega_{n,s}) \right]. \tag{7}$$

Figure 4 shows that all states are strongly localized, and the localization increases in the absence of *e-e* interactions. For $\eta = 1$, one recognizes that the least localized single particle wave functions are in the center of the Hubbard bands while the defect states at the edges of the Hubbard bands are stronger localized. A particularly interesting feature is the discontinuity of the IPN at the chemical

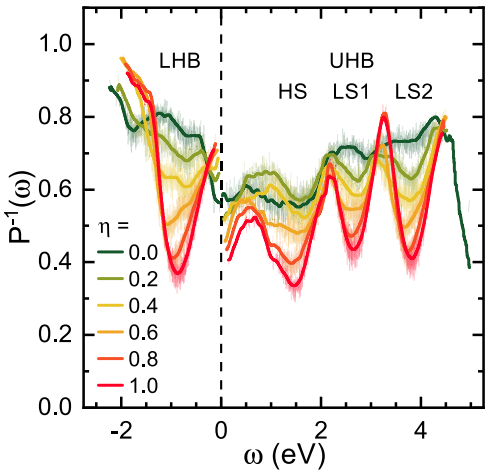

FIG. 4. Spectral functions $P^{-1}(\omega)$ (thick lines) and $P_n^{-1}\left(\langle\omega_{n,s}\rangle_s\right) = \left\langle P_{n,s}^{-1}\right\rangle_s$ (thin lines) representing the IPN obtained within the uHF approximation at $x = 0.10$ and for different η values. The smallest values of IPN coincide with the centers of the Hubbard bands, where the labels mark the LHB and the multiplet structure of the UHB, i.e., the high spin (HS) and the two low spin excitations (LS1, LS2). The chemical potential at $\omega = 0$ is marked by a dashed line.

potential (i.e. at $\omega = 0$). For $\eta \geq 0$ electron removal states below μ are more strongly localized in comparison to the electron addition states right above μ. Without $e - e$ interactions ($\eta = 0$), the discontinuity at μ appears to be absent. Such an high degree of localization provides an explanation for the persistence of spin and orbital order up to high doping.

IV. CONCLUSIONS

Summarizing, we note that the presence of the defect states gap for the model without *e-e* interactions is a feature unexpected on the basis of single orbital models. The linear gap for the case $\eta = 0$ is due to the kinetic energy of holes that move inside the spin-orbital polarons, along FM bonds. In a single orbital model with random levels, the kinetic energy leads to a mobility edge instead, whereas in a single orbital model with kinetic energy and *e-e* interactions, i.e., in the quantum CG, one expects that the kinetic energy tends to suppress the Coulomb gap. In the multi-orbital model for the vanadium perovskites instead, the kinetic energy and the *e-e* interactions cooperate in the formation of the defect states gap. Another interesting case is the atomic limit ($t \to 0$), which corresponds to the *classical* CG, for which Efros and Shklovskii[12] found a soft Coulomb gap with an exponent $\nu = d - 1$ determined uniquely by the spatial dimension. For the multi-band model studied here, we find in general non-universal exponents $\nu = k - 1$ determined by the Weibull distribution function of the minimal gap sampled over all defect realizations. In particular, we have reported earlier that, in the atomic limit of the multi-band model, there is no soft gap, but a Coulomb singularity $\nu < 1$, that is, *e-e* interactions alone are not strong enough in these compounds to develop a soft Coulomb gap.

ACKNOWLEDGMENTS

A.M.O. acknowledges support by Narodowe Centrum Nauki (NCN, Poland), Project No. 2016/23/B/ST3/00839.

[1] M. Imada, A. Fujimori, and Y. Tokura, Rev. Mod. Phys. **70**, 1039 (1998).
[2] S. Miyasaka, T. Okuda, and Y. Tokura, Phys. Rev. Lett. **85**, 5388 (2000).
[3] J. Fujioka, S. Miyasaka, and Y. Tokura, Phys. Rev. B **77**, 144402 (2008).
[4] M. Reehuis, C. Ulrich, P. M. Abdala, P. Pattison, G. Khaliullin, J. Fujioka, S. Miyasaka, Y. Tokura, and B. Keimer, Phys. Rev. B **94**, 104436 (2016).
[5] M. H. Sage, G. R. Blake, and T. T. M. Palstra, Phys. Rev. B **77**, 155121 (2008).
[6] G. Khaliullin, P. Horsch, and A. M. Oleś, Phys. Rev. Lett. **86**, 3879 (2001); Phys. Rev. B **70**, 195103 (2004).

[7] J. Fujioka, T. Yasue, S. Miyasaka, Y. Yamasaki, T. Arima, H. Sagayama, T. Inami, K. Ishii, and Y. Tokura, Phys. Rev. B **82**, 144425 (2010).
[8] P. Horsch and A. M. Oleś, Phys. Rev. B **84**, 064429 (2011).
[9] M. Daghofer, A. Nicholson, A. Moreo, and E. Dagotto, Phys. Rev. B **81**, 014511 (2010).
[10] A. Avella, P. Horsch, and A. M. Oleś, Phys. Rev. B **87**, 045132 (2013).
[11] A. Avella, A. M. Oleś, and P. Horsch, Phys. Rev. Lett. **115**, 206403 (2015); Physica B **536**, 738 (2018); Phys. Rev. B **97**, 155104 (2018).
[12] A. L. Efros and B. I. Shklovskii, J. Phys. C **8**, L49 (1975).
[13] M. Daghofer, K. Wohlfeld, A. M. Oleś, E. Arrigoni, and P. Horsch, Phys. Rev. Lett. **100**, 066403 (2008); P. Wróbel and A. M. Oleś, *ibid.* **104**, 206401 (2010).
[14] D. J. Thouless, Phys. Rep. **13**, 93 (1974); F. Epperlein, M. Schreiber, and T. Vojta, Phys. Rev. B **56**, 5890 (1997).